# Adsorption of Amphiphilic Diblock Copolymer Micelles at the Mica/Solution Interface

**ARTICLE** *in* LANGMUIR · SEPTEMBER 2001

Impact Factor: 4.46 · DOI: 10.1021/la010335+

# Adsorption of Amphiphilic Diblock Copolymer Micelles at the Mica/Solution Interface

Grant B. Webber,[†,‡] Erica J. Wanless,*[,†] Steven P. Armes,[§] Fiona L. Baines,[⊥] and Simon Biggs[†,‡]

*School of Biological and Chemical Sciences, The University of Newcastle, Callaghan, N.S.W., 2308 Australia; Centre for Multiphase Processes, The University of Newcastle, Callaghan, N.S.W., 2308 Australia; School of Chemistry, Physics and Environmental Science, University of Sussex, Falmer, Brighton BN1 9QJ, UK; and Unilever Research, Port Sunlight Laboratory, Quarry Road East, Bebington, Wirral CH63 3JW, UK*

*Received March 5, 2001. In Final Form: June 16, 2001*

The adsorption of the amphiphilic diblock copolymer poly(2-(dimethylamino)ethyl methacrylate-*block*-methyl methacrylate) (DMA−MMA) at the mica/solution interface has been studied, over a range of solution pH values, using in situ atomic force microscopy. In contrast to the adsorption of the homopolymer poly-(2-(dimethylamino)ethyl methacrylate (DMA), which exhibited a featureless adsorbed layer, adsorbed layers of the DMA−MMA copolymer exhibited lateral structure at all pH values studied. At low solution pH, images of the adsorbed layer reveal discrete domelike structures, separated by regions with no lateral features. Force−distance data recorded between these domes indicate adsorption in the form of positively charged material. It is proposed that the adsorbed layer forms via the adsorption of DMA−MMA micelles directly to the mica surface, followed by relaxation of the DMA chains to the surface. This relaxation is driven by electrostatics and results in an adsorbed layer that is essentially a layer of DMA chains with the MMA cores protruding as domes at the sites of the original micelle adsorption. The domes are evident over the entire surface, although arranged in a disordered manner. The distance between the domes is seen to decrease as the pH of the adsorbing copolymer solution is increased from 4 to 7, due to the increased number of negatively charged adsorption sites on the mica surface. Adsorption of charged latex particles shows that objects without molecular freedom adsorb in a close-packed manner. Close packing of adsorbed units is also observed when the DMA−MMA micelles are adsorbed from a solution at natural pH (pH 8.3), where the relaxation of the coronal DMA chains is electrostatically hindered.

## Introduction

Recently there has been increased interest in the adsorption of polyelectrolytes at solid/liquid interfaces due to their widespread and expanding technological application in industries such as wastewater treatment, cosmetics, and paints.[1,2] In particular, diblock copolymer polyelectrolytes have come under much greater investigation,[3−8] as the methodologies for synthesizing these molecules have advanced, thereby increasing the diversity of diblocks available. Amphiphilic diblock copolymers can exhibit a wide range of solution properties, since the overall amphiphilic nature of a molecule can be changed by judicious control of the polymer architecture. Of specific interest is the ability to control the amphiphilic nature of a particular diblock copolymer in solution through solution properties such as pH[9−11] or ionic strength.[10,12,13] It is this ability to change the nature of the copolymer while in solution (i.e., turn the amphiphilic nature "on" or "off") that has led to the application of these macromolecules in areas such as drug delivery, solubilization, nanostructure templates, and nanoreactors.

AB diblock copolymers have been the subject of research interest for many years, and their bulk solution properties have been extensively characterized.[9,10,12,14−17] In many instances, studies have concentrated on controlling the morphology of AB diblock copolymer aggregates in solution.[18−24] This is typically achieved either by changing

† School of Biological and Chemical Sciences, The University of Newcastle.
‡ Centre for Multiphase Processes, The University of Newcastle.
§ University of Sussex.
⊥ Port Sunlight Laboratory.
* Corresponding author: e-mail csew@paracelsus.newcastle.edu.au, phone 61-2-49218846, fax 61-2-49215472.

(1) Bremmel, K. E.; Jameson, G. J.; Biggs, S. *Colloids Surf.* **1998**, *139*, 199−211.
(2) Biggs, S.; Healy, T. W. *J. Chem. Soc., Faraday Trans.* **1994**, *90*, 3415−3421.
(3) Pina, A.; Nakache, E.; Feret, B.; Depraetere, P. *Colloids Surf.* **1999**, *158*, 375−384.
(4) Walter, H.; Harrats, C.; Muller-Buschbaum, P.; Jerome, R.; Stamm, M. *Langmuir* **1999**, *15*, 1260−1267.
(5) Kramer, E.; Forster, S.; Goltner, C.; Antonietti, M. *Langmuir* **1998**, *14*, 2027−2031.
(6) An, S. W.; Su, T. J.; Thomas, R. K.; Baines, F. L.; Billingham, N. C.; Armes, S. P.; Penfold, J. *J. Phys. Chem. B* **1998**, *102*, 387−393.
(7) Moffitt, M.; Eisenberg, A. *Macromolecules* **1997**, *30*, 4363−4373.
(8) Kelley, T. W.; Schorr, P. A.; Johnson, K. D.; Tirrell, M.; Frisbie, C. D. *Macromolecules* **1998**, *31*, 4297−4300.
(9) Webber, S. E. *J. Phys. Chem. B* **1998**, *102*, 2618−2626.
(10) Gohy, J. F.; Creutz, S.; Garcia, M.; Mahltig, B.; Stamm, M.; Jerome, R. *Macromolecules* **2000**, *33*, 6378−6387.
(11) Martin, T. J.; Prochazka, K.; Munk, P.; Webber, S. E. *Macromolecules* **1996**, *29*, 6071−6073.
(12) Gast, A. P. *Curr. Opin. Colloid Interface Sci.* **1997**, *2*, 258−263.
(13) Guenoun, P.; Davis, H. T.; Tirrell, M.; Mays, J. W. *Macromolecules* **1996**, *29*, 3965−3969.
(14) Esselink, F. J.; Dormidontova, E. E.; Hadziioannou, G. *Macromolecules* **1998**, *31*, 4873−4878.
(15) Stepanek, M.; Podhajecka, K.; Prochazka, K.; Teng, Y.; Webber, S. E. *Langmuir* **1999**, *15*, 4185−4193.
(16) Hickl, P.; Ballauff, M.; Jada, A. *Macromolecules* **1996**, *29*, 4006−4014.
(17) Cox, J. K.; Yu, K.; Constantine, B.; Eisenberg, A.; Lennox, R. B. *Langmuir* **1999**, *15*, 7714−7718.
(18) Baines, F. L.; Armes, S. P.; Billingham, N. C.; Tuzar, Z. *Macromolecules* **1996**, *29*, 8151−8159.
(19) Butun, V.; Billingham, N. C.; Armes, S. P. *Chem. Commun.* **1997**, 671−672.
(20) Lowe, A. B.; Billingham, N. C.; Armes, S. P. *Chem. Commun.* **1997**, 1035−1036.
(21) De Paz Banez, M. V.; Robinson, K. L.; Armes, S. P. *Macromolecules* **2000**, *33*, 451−456.

10.1021/la010335+ CCC: $20.00 
Published on Web 07/27/2001

the copolymer architecture or through alterations to the solvent properties. Eisenberg and co-workers have undertaken a detailed investigation of changing aggregate morphology of polystyrene-*block*-poly(acrylic acid) (PS-*b*-PAA) aggregates.[25−28] In these studies, changes in the type of solution aggregates formed have been induced both through changes in the relative mass ratio of the two polymer blocks and by changing the chemical composition of the solvent. Despite the strong interest in AB diblock copolymer micelles, there are few reports of the adsorption of copolymer micelles at the solid/liquid interface. Instead, in most cases, surface films have been prepared by annealing, or solvent-drying techniques, with the dried sample then examined using transmission electron microscopy (TEM)[29−32] or atomic (scanning) force microscopy (AFM)[33−37] in air.

Dried films of adsorbed copolymer have been found to retain some of the key characteristics of the parent solution, particularly those reflecting solvent qualities. Breulman et al.[29] used TEM to study copolymers based on polystyrene-*block*-polybutadiene (PS-*b*-PBD), with the PBD block modified to contain alcohol or carboxylate groups. Toluene solutions of these block copolymers result in micelles with a polystyrene shell and a hydroxylic or acid-block core. The authors found that the 2-dimensional surface pattern formed by these copolymers on a carbon-coated copper grid was dependent on the relative size of the soluble and insoluble blocks. As the relative amount of the insoluble block is increased, a transition from spherical domains to striped domains occurs, with phase inversion eventually possible if the amount of insoluble block exceeds that of the soluble block. Yu et al.[30] observed similar results when examining films of the block copolymer polybutadiene-*block*-poly(acrylic acid) (PBD-*b*-PAA). Micellar solutions of the copolymer were prepared by dissolving the copolymer in toluene, a good solvent for both blocks, and then adding deionized water, producing micelles with a core of PBD and shell of PAA. By varying the relative amounts of PBD and PAA, the authors observed rodlike aggregates, vesicles, ribbonlike aggregates, and large compound micelles in the films cast from the micellar solutions. Scanning force microscopy (SFM) was used by Potemkin et al.[33] to image dried layers of polystyrene-*block*-poly(2-vinylpyridine) (PS-*b*-P2VP) on mica. In this case, the copolymer was dissolved in chloroform, which is a nonselective solvent for both blocks. The authors found that by varying the relative amounts of the PS and P2VP blocks the dried layers varied from structures with circular projection to structures with an elongated, wormlike projection. In contrast to this work is an SFM study by Spatz et al.[34] into films formed by PS-*b*-P2VP in the selective solvent toluene. SFM and TEM were used to image dried layers of PS-*b*-P2VP on mica and carbon-coated copper grids, respectively. It was shown that, by increasing the concentration of the copolymer in the solution, a change from structures with circular to wormlike projections occurred.

Recently, the application of AFM techniques to in situ investigations of the adsorption of molecules and aggregates at the solid/liquid interface has been demonstrated. In particular, in situ measurements of adsorbed layer structures formed by small molecule surfactants have received much attention.[38−41] However, to the authors' best knowledge, only one previously published study, by Regenbrecht et al.,[42] has used in situ AFM to study the adsorption of diblock copolymer micelles. Their study investigated the adsorption of the negatively charged AB diblock copolymer poly(ethylene-*block*-styrenesulfonic acid) on graphite surfaces as a function of salt concentration and compared the images with those taken using dried samples of the same solutions. They concluded that there was little change in surface aggregate morphology when the adsorbed layer was dried, though it is not possible to conclude whether this result is specific to the system or representative of diblock copolymer systems in general.

The advantages of studying the adsorption of diblock copolymer micelles using in situ AFM are many. The variety of surfaces that may be used in the AFM cell is only limited by the surface roughness of the material, with silica, muscovite mica, and graphite among the most frequently used, although it is also possible to use chemically modified surfaces.[43,44] In situ AFM also allows the kinetics of adsorption of diblock micelles at the surface to be monitored over time, with the distinct advantage that the same section of surface may be studied throughout the experiment. Of course, the main advantage of using in situ AFM is that it eliminates any possible changes in the structure of the adsorbed layer as a result of the drying process that is integral to either TEM (in vacuo) or AFM in air. Therefore, the images of the adsorbed layer, and indeed the force−distance data measured normal to the layer, are more representative of the natural adsorption conditions in the presence of the bulk solution. The main limitation of using in situ AFM to image a layer of absorbed material is that the cantilever tip is in contact with the layer during the imaging process. However, if a long-range repulsive interaction exists between the tip and the layer, it is possible to scan the surface with the tip at a small distance from the surface. By utilizing this distinct noncontact repulsive force, as opposed to the Born repulsive force, imaging exerts minimal force on the

(22) Lowe, A. B.; Bilingham, N. C.; Armes, S. P. *Macromolecules* **1998**, *31*, 5991−5998.
(23) Yu, K.; Eisenberg, A. *Macromolecules* **1996**, *29*, 6359−6361.
(24) Baines, F. L.; Billingham, N. C.; Armes, S. P. *Macromolecules* **1996**, *29*, 3416−3420.
(25) Zhang, L.; Eisenberg, A. *Science* **1995**, *268*, 1728−1731.
(26) Zhang, L.; Hongwei, S.; Eisenberg, A. *Macromolecules* **1997**, *30*, 1001−1011.
(27) Yu, Y.; Eisenberg, A. *J. Am. Chem. Soc.* **1997**, *119*, 8383−8384.
(28) Zhang, L.; Eisenberg, A. *J. Am. Chem. Soc.* **1996**, *118*, 3168−3181.
(29) Breulmann, M.; Forster, S.; Antonietti, M. *Macromol. Chem. Phys.* **2000**, *201*, 204−211.
(30) Yu, Y.; Zhang, L.; Eisenberg, A. *Langmuir* **1997**, *13*, 2578−2581.
(31) Yokoyama, H.; Mates, T. E.; Kramer, E. J. *Macromolecules* **2000**, *33*, 1888−1898.
(32) Meiners, J. C.; Quintelritzi, A.; Mlynek, J.; Elbs, H.; Krausch, G. *Macromolecules* **1997**, *30*, 4945−4951.
(33) Potemkin, I. I.; Kramarenko, E. Y.; Khokhlov, A. R.; Winkler, R. G.; Reineker, P.; Eibeck, P.; Spatz, J. P.; Moller, M. *Langmuir* **1999**, *15*, 7290−7298.
(34) Spatz, J. P.; Sheiko, S.; Moller, M. *Macromolecules* **1996**, *29*, 3220−3226.
(35) Regenbrecht, M.; Akari, S.; Forster, S.; Mohwald, H. *J. Phys. Chem. B* **1999**, *103*, 6669−6675.
(36) Stapff, I.; Weidemann, G.; Schellenberg, C.; Regenbrecht, M.; Akari, S.; Anonietti, M. *Surf. Interface Anal.* **1999**, *27*, 392−395.
(37) Regenbrecht, M.; Akari, S.; Forster, S.; Mohwald, H. *Surf. Interface Anal.* **1999**, *27*, 418−421.
(38) Velegol, S. B.; Fleming, B. D.; Biggs, S.; Wanless, E. J.; Tilton, R. D. *Langmuir* **2000**, *16*, 2548−2556.
(39) Manne, S.; Cleveland, J. P.; Gaub, H. E.; Stucky, G. D.; Hansma, P. K. *Langmuir* **1994**, *10*, 4409−4413.
(40) Wanless, E. J.; Ducker, W. A. *J. Phys. Chem.* **1996**, *100*, 3207−3214.
(41) Patrick, H. N.; Warr, G. G.; Manne, S.; Aksay, I. A. *Langmuir* **1999**, *15*, 1685−1692.
(42) Regenbrecht, M.; Akari, S.; Forster, S.; Netz, R. R.; Mohwald, H. *Nanotechnology* **1999**, *10*, 434−439.
(43) Noy, A.; Frisbie, C. D.; Rozsnyai, L. F.; Wrighton, M. S.; Lieber, C. M. *J. Am. Chem. Soc.* **1995**, *117*, 7943−7951.
(44) Ito, T.; Namba, M.; Buhlmann, P.; Umezawa, Y. *Langmuir* **1997**, *13*, 4323−4332.

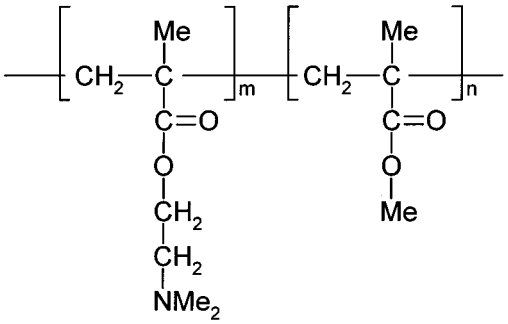

**Figure 1.** Molecular structure of the poly(2-(dimethylamino)-ethyl methacrylate-*block*-methyl methacrylate) (DMA−MMA) copolymer.

adsorbed layer, thus reducing the potential for perturbations of the adsorbed layer.[45,46]

In this article we present an in situ investigation of the amphiphilic diblock copolymer poly(2-(dimethylamino)-ethyl methacrylate-*block*-methyl methacrylate) (DMA−MMA) adsorbed from an aqueous solution onto a muscovite mica substrate. The diblock copolymer consists of one permanently hydrophobic block (MMA) and one block that can be made either hydrophilic or hydrophobic by changing the pH of the solution (DMA). The molecular structure of DMA−MMA is shown in Figure 1. This copolymer has been shown to form micellar aggregates in solution under certain conditions,[18] and we therefore anticipate interesting adsorption behavior. The adsorption of DMA homopolymer, a positively charged polyelectrolyte, and of positively charged latex particles was also studied using in situ AFM to aid in the understanding of the adsorption of the DMA−MMA copolymer. Dynamic light scattering (DLS) was employed to monitor the size of the DMA−MMA micelles in bulk solution, so that the bulk solution properties could be related to the observed adsorbed layer morphology.

## Experimental Section

**Materials.** Poly(2-(dimethylamino)ethyl methacrylate) (DMA) was synthesized using group transfer polymerization, the details of which are described elsewhere.[24] The DMA used in this study had a molecular weight of 13 300 g mol$^{-1}$ and a $M_w/M_n$ of 1.08. The solutions were prepared by dissolving the requisite amount of the homopolymer in a small amount of methanol (BDH, AR Grade, used without further purification) and then diluting with Milli-Q grade water to a final solvent mixture of 4/96% w/w methanol/water. The solutions were then adjusted to pH 4 by addition of small amounts of concentrated nitric acid (Ajax Chemicals, AR Grade).

Synthetic details for the diblock copolymer poly(2-(dimethylamino)ethyl methacrylate-*block*-methyl methacrylate) (DMA−MMA) have also been reported elsewhere.[24] The hydrophilic−hydrophobic block copolymer was synthesized using group transfer polymerization, had a molecular weight of 42 800 g mol$^{-1}$, contained 79% DMA, and had a $M_w/M_n$ of 1.15. Solutions of the diblock copolymer were also prepared by weighing out an appropriate amount of the copolymer and then dissolving in a small amount of methanol. The solution was then diluted with Milli-Q grade water to a final solvent mixture of 4/96% w/w methanol/water. Where necessary, pH was adjusted by additions of small quantities of concentrated nitric acid. Potassium nitrate (Ajax Chemicals, AR Grade) was used with no further purification. This was added to give a background electrolyte concentration of $10^{-2}$ M. The copolymer solutions were prepared the day before they were used in experiments so that solution equilibrium was reached. A concentration of 500 ppm DMA−MMA was used for both the AFM and DLS experiments.

Amidinated positively charged hydrophobic latex spheres were obtained from Interfacial Dynamics Corp. (Portland, OR). The spheres had a quoted diameter of 0.027 $\mu$m with a 21.7% coefficient of variation (standard deviation/mean diameter) and were supplied as a 4.3% solids aqueous solution. This solution was diluted with Milli-Q grade water to a 4.3 ppm solution before use in AFM experiments.

**Atomic Force Microscopy.** A Nanoscope III AFM (Digital Instruments, CA) was used for in situ imaging of the adsorbed layer and for recording force profiles. Cantilevers having an integral silicon nitride tip (NanoProbe, Digital Instruments, CA) were used for all AFM experiments. These cantilevers were cleaned prior to use by irradiation using UV light (approximately 9 mW/cm$^2$ at 253.7 nm) for 30 min in a laminar flow cabinet. The spring constant of the cantilevers was determined by the method of Cleveland et al.[47] to be 0.059 N m$^{-1}$. The muscovite mica substrate was freshly cleaved in a laminar flow cabinet before use. All solutions were passed through a syringe-mounted 0.2 $\mu$m filter (GHP Acrodisc, Pall Gelman Sciences, MI) as they were injected into the AFM fluid cell. All images presented are deflection images, except those of the latex spheres (Figure 10) which are height images. All images presented have been zero-order flattened. Images were taken using the soft-contact imaging technique,[45] which uses the minimum force possible to image the adsorbed layer, to maintain the morphology of the adsorbed layer.

At the start of each AFM experiment Milli-Q water, at the same pH as the copolymer solution to be studied, was injected into the fluid cell of the AFM. The water was left in the cell for approximately 20−30 min, to allow the mica surface to equilibrate to the pH and to also image the surface to verify that the mica was free of contaminants. At this point the copolymer solution was injected into the fluid cell, and images of the adsorbed layer, and interaction force data, were taken periodically for the next 20−24 h.

**Dynamic Light Scattering.** An ALV/DLS/SLS-5022F light scattering instrument (ALV, Germany) was used in this study. The hydrodynamic radius ($R_H$) for each sample was measured at different angles from 90° to 30°. Very little angular dependence was exhibited for any of the samples, and thus only the hydrodynamic radius values measured at 90° are quoted. These $R_H$ values were calculated using a second-order cumulant fit of the scattering data. In this method the measured correlation function is fitted using the equation

$$\ln(g_1(t)) = \ln(A) - \Gamma t + \frac{\mu_2}{2} t^2 \quad (1)$$

where $A$ and $\mu_2$ are fitting parameters and $\Gamma$ is the decay rate. The hydrodynamic radius is then calculated using the Stokes−Einstein equation:

$$R_H = \frac{kT}{6\pi\eta\Gamma} q^2 \quad (2)$$

where $k$ is the Boltzmann constant, $T$ is the temperature, $\eta$ is the solvent viscosity, and $q$ is the magnitude of the scattering vector. The scattering vector is given by

$$q = \frac{4\pi n}{\lambda} \sin(\theta/2) \quad (3)$$

where $n$ is the solvent refractive index, $\lambda$ is the wavelength of incident laser light, and $\theta$ is angle at which the scattered light was measured.

All solutions were filtered through 0.2 $\mu$m syringe-mounted filters as they were injected into the light scattering cell. To aid in the removal of impurities in these copolymer solutions, all solvents were similarly filtered during the preparation of the solutions.

(45) Fleming, B. D.; Wanless, E. J. *Microsc.Microanal.* **2000**, *6*, 104−112.

(46) Senden, T. J.; Drummond, C. J.; Kekicheff, P. *Langmuir* **1994**, *10*, 358−362.

(47) Cleveland, J. P.; Manne, S.; Bocek, D.; Hansma, P. K. *Rev. Sci. Instrum.* **1993**, *64*, 403−405.

## Results and Discussion

**DMA Homopolymer Adsorption.** When the DMA−MMA copolymer forms micelles in solution, the charged DMA chains form the corona, and so adsorption of DMA−MMA micelles is likely to occur as a result of DMA chain adsorption. A DMA homopolymer was thus studied in situ using atomic force microscopy to characterize the adsorption of the charged chains on muscovite mica, without the complication of the MMA block. All solutions of DMA homopolymer were adjusted to a pH of 4, ensuring a net positive charge on the tertiary amine groups of the DMA chains. Homopolymer adsorption was studied in two ways: (1) by adsorption of a 5 ppm DMA solution onto a freshly cleaved piece of mica, followed by sequential injections of 10, 50, and 250 ppm DMA solutions, allowing at least 2 h between successive solutions, and (2) by direct adsorption of a 250 ppm DMA solution onto a freshly cleaved piece of mica. Images of the adsorbed DMA homopolymer are shown in Figure 2 for both modes. In all cases the homopolymer adsorbed as a featureless layer that completely coated the mica. No evidence for any lateral structure was observed.

Force−distance data for the interaction between the cantilever tip and the adsorbed DMA layer were also recorded for each DMA solution and are shown in Figures 3 and 4. These data indicate an interesting difference between the two experimental modes detailed above that is not apparent in the images of the adsorbed layers. In Figure 3, the data for the bare mica substrate and the cantilever tip at pH 4 indicate a weak electrostatic attraction. This is expected for a negative mica surface and a positive silicon nitride tip.[48] Upon injection of the 5 ppm DMA solution into the liquid cell, the DMA chains are expected to adsorb to the mica surface through electrostatic attraction. The resultant force−distance data are also attractive, although both the depth of the attractive minimum and the distance over which it acts are seen to increase. This is attributed to the formation of a flat uncharged polymer layer at the surface due to the efficient neutralization of the mica surface charge as the polymer adsorbs. Such a layer may be expected to have considerable hydrophobic character. Previous studies[49−51] have shown that the interaction of a hydrophilic surface, in this case the cantilever tip, with a hydrophobic one, the adsorbed polymer layer, can lead to significant attractive interactions, as seen here. The subsequent injection of the 10 ppm solution indicates further DMA adsorption onto the mica surface as evidenced by the increases in the range and strength of the attractive force. It can be seen from Figure 3 that subsequent injections of solutions with higher DMA concentrations has no further influence on the magnitude of the hydrophobic attraction force between the tip and the surface. Thus, sufficient DMA adsorption for charge neutralization of the mica surface was achieved at 10 ppm DMA.

The force data measured when the DMA sample was introduced to a clean mica substrate at a solution concentration of 250 ppm solution are shown in Figure 4. In this case a purely repulsive interaction is evident between the tip and the adsorbed layer. The origin of this repulsion is attributed to an electrosteric interaction caused by the expanded adsorbed layer of the DMA. The high DMA concentration in solution leads to rapid adsorption. This prevents significant lateral relaxation of any DMA chains and leads to an extended loops and tail conformation, which results in a longer range repulsive force.[1]

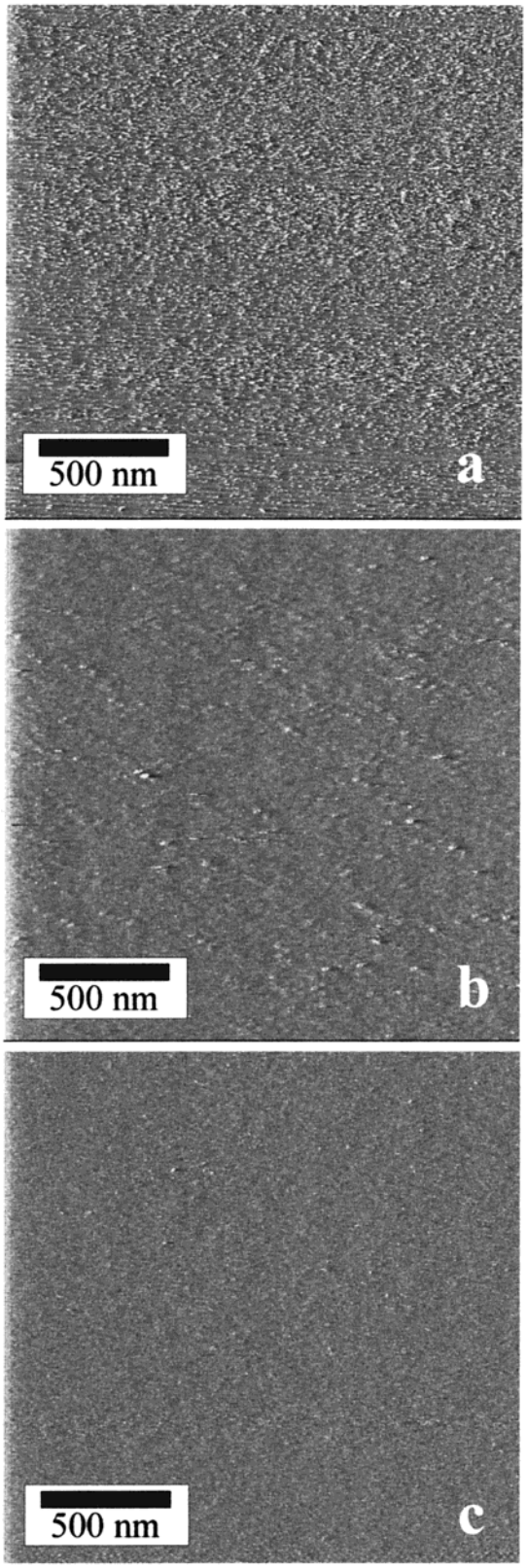


**Figure 2.** AFM soft-contact deflection images of (a) 5 ppm DMA homopolymer solution adsorbed to a clean mica surface, (b) 250 ppm DMA solution adsorbed to mica following adsorption from a lower concentration of DMA homopolymer, and (c) 250 ppm DMA homopolymer solution adsorbed directly to a clean mica surface.

(48) Senden, T. J.; Drummond, C. J. *Colloids Surf.* **1995**, *94*, 29−51.
(49) Rabinovich, Y. I.; Yoon, R.-H. *Colloids Surf.* **1994**, *93*, 263−273.
(50) Rabinovich, R. I.; Yoon, R.-H. *Langmuir* **1994**, *10*, 1903−1909.
(51) Mantel, M.; Rabinovich, Y. I.; Wightman, J. P.; Yoon, R.-H. *J. Colloid Interface Sci.* **1995**, *170*, 203-214.

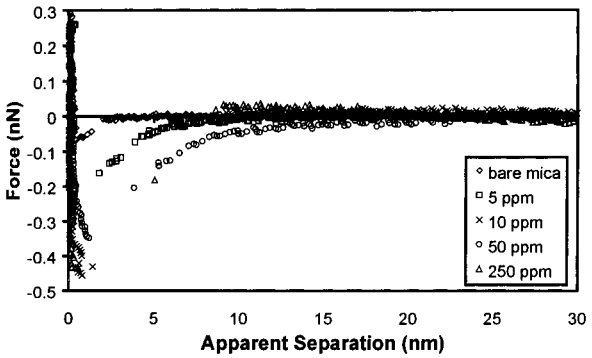


**Figure 3.** Forces normal to the surface measured following successive injections of DMA homopolymer solutions of increasing concentration. An equilibration time of at least 2 h was allowed before injecting each more concentrated solution.

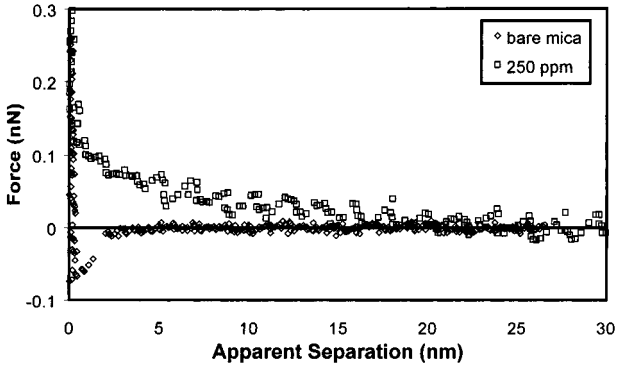


**Figure 4.** Forces normal to the surface measured in a 250 ppm DMA homopolymer solution adsorbed directly onto a freshly cleaved mica surface.

**DMA−MMA Copolymer Adsorption.** The adsorption of DMA−MMA from a 500 ppm solution at pH 4 onto a mica substrate was monitored in situ using atomic force microscopy. Images of the surface were taken over a 22 h period after the initial injection of the copolymer solution as shown in Figure 5. These images are representative of the entire sample and clearly show the presence of adsorbed structures not observed for the homopolymer sample. Also, these surface structures increase in number as a function of time. The surface structures are of uniform size and are discrete units. DMA−MMA copolymer chains are known to form micellar aggregates in acidic solution.[18] The micelles have a MMA core and DMA corona, due to the protonation of the tertiary amine groups on the DMA segments rendering the copolymer chains amphiphilic. The surface structures seen in the images are therefore likely to arise directly from copolymer micelles adsorbed from solution onto the mica surface.

Force−distance data were also recorded "on" the structure, Figure 6, and in the interstructure areas, Figure 7. Of note is the fact that the force curve between the bare mica surface and the cantilever tip always shows a weak electrostatic attraction, indicating that there should be minimal adsorption of the positively charged DMA−MMA copolymer chains to the similarly charged tip. Upon addition of the copolymer chains the force−distance data become purely repulsive, both "on" a structure and in the interstructure regions, and remain that way throughout the 22 h period. This is convenient as it allows imaging of the surface to be done in a repulsive region of the force−distance profile at a finite separation, which is known as soft-contact imaging.[38,39,45] Imaging the adsorbed copolymer layer in his manner minimizes any deformation of the surface morphology due to the scanning motion of the tip. Because of inherent drift in the piezo of the AFM scanner and the difficulties associated with maintaining a centered structure when zooming, it is not possible to state definitively that the "on" structure force curves are recorded with the cantilever tip directly above a structure. Also, as the number of adsorbed structures increases, it becomes increasingly difficult to find an interstructure area large enough to record definitively off-structure force−distance data.

If the adsorbed structures are indeed adsorbed copolymer micelles, then one would expect force curves measured above these structures to show an electrostatic repulsion due to the interaction of the positively charged tip and the positively charged DMA chains of the micelle corona. This is observed. The force data also show a steeply repulsive region at approximately 1−2 nm from the apparent zero separation point, followed by an inward jump at around 0.5−1 nm, which is not seen in the force data from the interaggregate areas. This may indicate that the tip is indeed above an aggregate. We postulate that this steep region in the data occurs as a result of the tip pushing against the glassy MMA core. The small jump-in may then result as the tip pushes into the core toward the surface. Exact interpretation of force−distance data using an AFM is difficult due to uncertainties in the zero separation distance. This is especially so when adsorbed polymers are present.[2,52] Despite this, much interesting information may still be inferred qualitatively about adsorbed layer conformation and changes within a system as conditions are altered.

Interestingly, the force data measured in the interstructure areas also become, and then remain, purely repulsive after the adsorption of the copolymer layer. If the DMA−MMA micelles adsorbed to the surface and remained in the same conformation as in solution, then one would expect that the areas between the structures to retain an attractive force curve, indicative of bare mica. The repulsive force data measured in the interstructure regions indicate that there has in fact been adsorption in these areas, although this is not readily apparent in the images (Figure 5). The force curves in the interstructure regions also exhibit a jump in at the short time frames of up to 1 h, after which the force curves remain repulsive at all separations.

**Model of DMA−MMA Micelle Adsorption to a Solid Surface.** The surface structures in the adsorbed layer of DMA−MMA copolymer on mica observed by in situ AFM may be formed in one of two possible ways. They could be formed on the surface, either as a result of surface rearrangements of adsorbed copolymer chains or by the action of the tip scanning across the surface during imaging, or the structures could be micelles adsorbed directly from solution onto the mica surface. Of these two possible methods, the first would result in structures of varied shapes and sizes, while the images in Figure 5 clearly show that the structures in the adsorbed layer are uniform in morphology.

It is thus proposed that the copolymer DMA−MMA adsorbs from solution to a mica surface via the direct adsorption of DMA−MMA micelles from the bulk solution. The adsorption of DMA−MMA micelles is driven by the electrostatic interactions between the positively charged micelle corona and the negatively charged mica surface. Once adsorbed to the surface, it is proposed that the previously spherical copolymer micelle undergoes a structural change, which leads to the spreading of the micelle across the surface. This rearrangement occurs as result

(52) Biggs, S. *Langmuir* **1995**, *11*, 156−162.

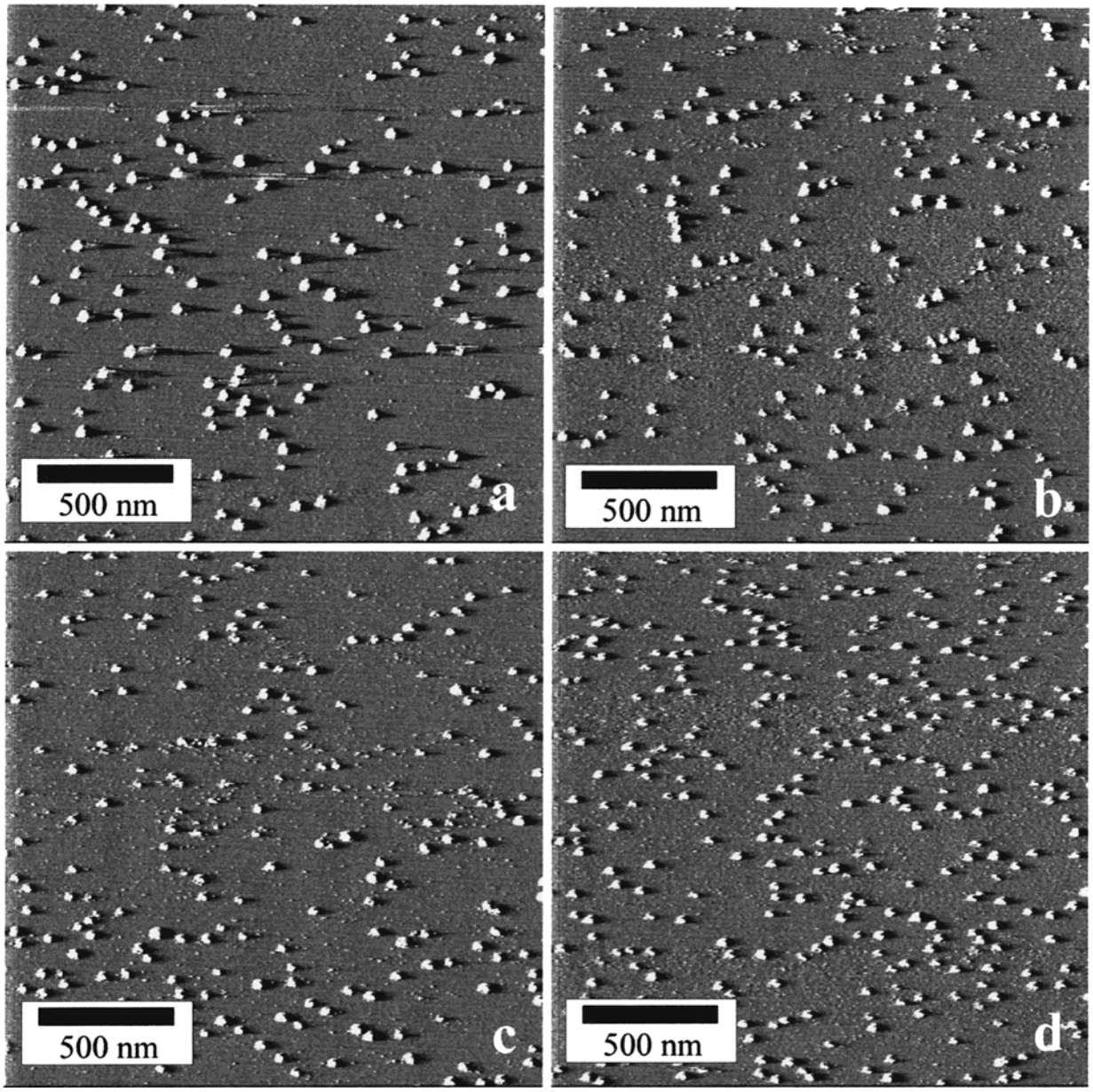


**Figure 5.** Images of the adsorbed layer (a) 5 min, (b) 1 h, (c) 5 h, and (d) 22 h after the injection of a 500 ppm DMA−MMA copolymer solution at pH 4.

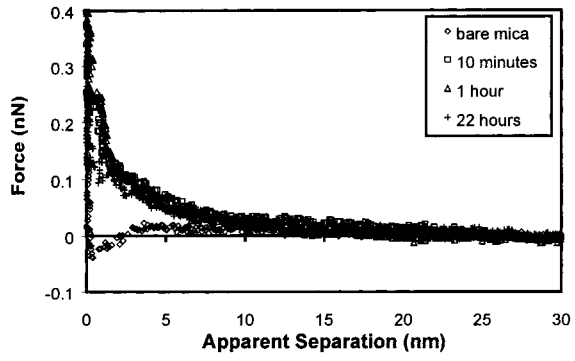


**Figure 6.** Force vs apparent separation measured "on" an aggregate in the copolymer layer adsorbed from a 500 ppm DMA−MMA solution onto a mica surface.

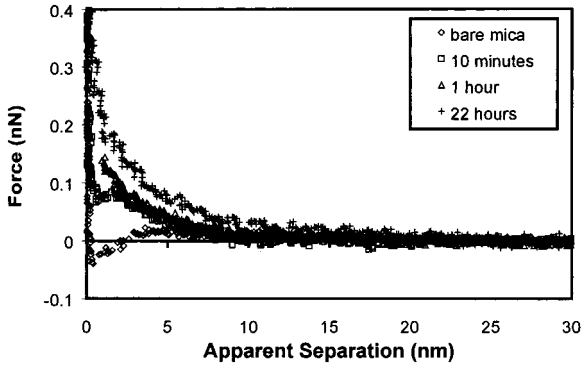


**Figure 7.** Force vs apparent separation measured in the interaggregate areas of the copolymer layer adsorbed from a 500 ppm DMA−MMA solution onto a mica surface.

of electrostatic interactions between the surface and the charged DMA coronal chains. A schematic representation for this model of DMA−MMA copolymer adsorption onto a mica surface is shown in Figure 8.

The proposed model of adsorption results in complete substrate coverage with an adsorbed layer of copolymer that is locally inhomogeneous. The model consists essentially of freely adsorbed DMA chains with localized

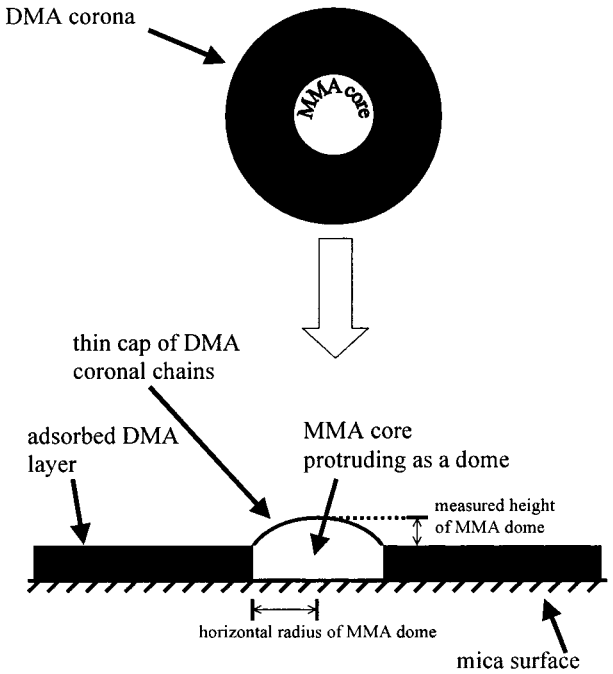


**Figure 8.** Schematic representation of the adsorption of a DMA−MMA copolymer micelle from a 500 ppm solution onto a mica surface.

cores of MMA embedded within the layer at the sites of the initial DMA−MMA micelle adsorption. When an image of the adsorbed layer is recorded using in situ AFM, the image reveals the glassy MMA cores as domes protruding from a featureless DMA layer. Force−distance data indicate that the MMA core is still coated in a charged DMA layer (Figure 6). The proposed adsorption mechanism would also result in the areas between the MMA cores having an adsorbed layer of DMA chains similar to that found for the adsorption of DMA homopolymer at 250 ppm. The force−distance data given in Figure 7 reveal the presence of an electrosteric layer, supporting this hypothesis.

Talingting et al.[53] proposed a similar mechanism for the adsorption of cationic micelles of polystyrene-*block*-poly(2-vinylpyridine) (PS−P2VP) onto an anionic poly(styrenesulfonate) layer, in which they postulate the possibility of the charged P2VP chains folding down onto the surface. Their argument was based on the two-dimensional distribution of the adsorbed micelles, which also indicates that the effective radius of the adsorbed micelles are significantly larger than their radius in solution. Also, the height profile of the adsorbed layer measured by AFM shows that the heights of the adsorbed aggregates are smaller than the diameter of micelles in solution. These conclusions must be qualified, however, since the images were taken of dried adsorbed layers.

Height images of the adsorbed DMA−MMA copolymer layer were recorded, from which the vertical heights and horizontal radii of the MMA domes were measured. It should be noted here that the vertical height measured is not the true height of the dome above the mica surface. Rather, it is the difference between the height of the MMA dome above the mica and the thickness of the surrounding DMA layer, as per Figure 8. The average vertical height of the aggregates measured over five different images was 5.2 ± 1.3 nm and the average horizontal radius 36.3 ± 14.8 nm. If one assumes that the MMA dome protruding from the surrounding DMA layer can be represented by a segment of a sphere, then the volume of the dome is given by

$$V = \frac{1}{6}\pi h(3r^2 + h^2) \tag{4}$$

where $h$ is the height of the MMA dome and $r$ is the radius of the circular base of the MMA dome. Using the above formula, and the average values of height and radius of the MMA domes, the dome volume was found to be $1.09 \times 10^4$ nm$^3$. It should be noted here that the horizontal radius of the MMA dome measured using the AFM is likely to be an overestimate, due to convolutions between the cantilever and the MMA dome, whereby the image of the dome is broadened due to the finite dimensions of the tip. Consequently, the calculated volume will also be an overestimate. However, compounded with this is the unknown volume of the MMA core lying embedded in the DMA layer. The inward jump in the force−distance data displayed in Figure 7 indicate that the thickness of the DMA layer is likely to be of the order of a few nanometers. Thus, the volume of the MMA core embedded in the DMA layer is likely to be small relative to the volume of the dome.

The hydrodynamic radius, $R_H$, of the DMA−MMA copolymer micelles in a 500 ppm solution was measured using dynamic light scattering. Assuming that the copolymer forms spherical micelles, the measured $R_H$ of 30.46 ± 0.86 nm gives a micellar volume of $1.18 \times 10^5$ nm$^3$, an order of magnitude greater than the volume calculated for the MMA dome protruding from the surrounding DMA layer. Given that the calculated volume for the MMA dome is likely to be an overestimate, the difference between the two volumes is significant. Even allowing for the unknown volume of the MMA core embedded in the DMA layer, this result indicates that the domes in the adsorbed copolymer layer are not large enough to be an entire micelle. Thus, the domes are assumed to be MMA cores, protruding from a surrounding layer of relaxed DMA coronal chains.

Given that the micelles of DMA−MMA appear to adsorb at the mica surface as discrete units in a random fashion, the kinetics of adsorption was investigated using a counting method, similar to that of Johnson and Lenhoff.[54] In their work, Johnson and Lenhoff studied the kinetics of latex particle adsorption by counting the number of adsorbed particle centers per unit area from AFM images as a function of time. Here, we use a similar approach, by counting the number of MMA domes imaged per unit area, and assuming that each MMA dome represents the site of adsorption for only one DMA−MMA copolymer micelle. The number of MMA domes per unit area was measured in two different ways. In the first method a 2 $\mu$m × 2 $\mu$m image was divided into four 1 $\mu$m$^2$ areas, and the mean number of MMA domes per square micron was determined. In the second method, four 1 $\mu$m$^2$ areas were taken from random positions on a 10 $\mu$m × 10 $\mu$m image. The mean number of MMA domes per square micron was then determined. In Figure 9, data for the number of MMA domes as a function of time using the two analysis routes are shown. These data show an increase in the number of MMA domes per square micron over the first 2−3 h, followed by a slower buildup during the remainder of the 22 h period. Some of the scatter in these data can be explained by the inherent drift in the piezo over the course of any experiment, making it difficult to image precisely the same area of surface each time.

(53) Talingting, M. R.; Ma, Y.; Simmons, C.; Webber, S. E. *Langmuir* **2000**, *16*, 862−865.

(54) Johnson, C. A.; Lenhoff, A. M. *J. Colloid Interface Sci.* **1996**, *179*, 587−599.

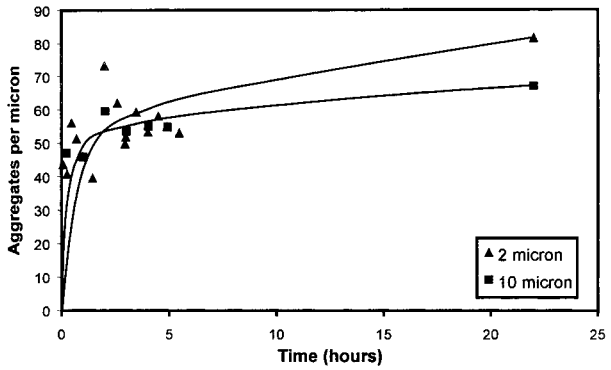


**Figure 9.** Kinetics of DMA−MMA copolymer adsorption from a 500 ppm solution measured from the AFM images via a counting method. The lines do not represent an actual fit of the data and are intended merely to show the inherent trends.

From the counted number of MMA domes per square micron, it is also possible to determine the effective "footprint" of the adsorbed DMA−MMA micelles, that is, the area each collapsed micelle occupies on the surface. This is only possible if one assumes that each imaged MMA dome represents the site of adsorption for only one micelle. The number of domes per micron after 22 h is approximately between 65 and 80, from the 2 $\mu$m × 2 $\mu$m and 10 $\mu$m × 10 $\mu$m images, respectively. This equates to a surface area of between 12 500 and 15 400 nm$^2$, which gives a radius of 63−70 nm if one assumes the adsorbed area to be circular. Given that the DMA−MMA micelles have an $R_H$ of 30.46 nm, it is clear that the micelles spread and flatten considerably once they are adsorbed to the mica.

**Latex Particle Adsorption.** To further investigate the role of molecular freedom in the adsorption of DMA−MMA micelles, the adsorption of a small positively charged latex sample onto mica was examined. The latex sample is nondeformable, and as such, its adsorption is not complicated by structural changes during or after adsorption. Height images were taken of the latex particles adsorbed from 4.3 and 43 ppm solutions and are shown in Figure 10. When the latex is adsorbed from the lower concentration solution, only a few latex spheres are seen in the images of the surface. When adsorbed from the higher concentration, the latex spheres entirely cover the mica surface. Force curves taken in areas of the surface well displaced from the latex particles absorbed from the 4.3 ppm solution show a similar interaction to that of the tip and a bare mica surface. This indicates that there is no adsorption in the regions between the latex particles, as expected. Since there is no adsorption in these regions, the surface still has a large number of charged sites available for adsorption. Consequently, when the higher concentration latex sample is injected into the fluid cell, the latex particles adsorb at the exposed charged sites and more efficiently cover the surface. This result shows that a solution of nondeformable charged particles will rapidly cover a mica surface, with the individual latex particles adsorbing in a random, closely packed configuration. This result is consistent with the data presented by Johnson and Lenhoff.[54] In the case of DMA−MMA micelles, which have molecular freedom, the MMA domes are well separated from each other even at an order of magnitude higher concentration. This is due to the relaxation of the DMA coronal chains after adsorption, which neutralizes charged sites on the surface and thus prevents further adsorption of a DMA−MMA micelle close to a previously adsorbed micelle.

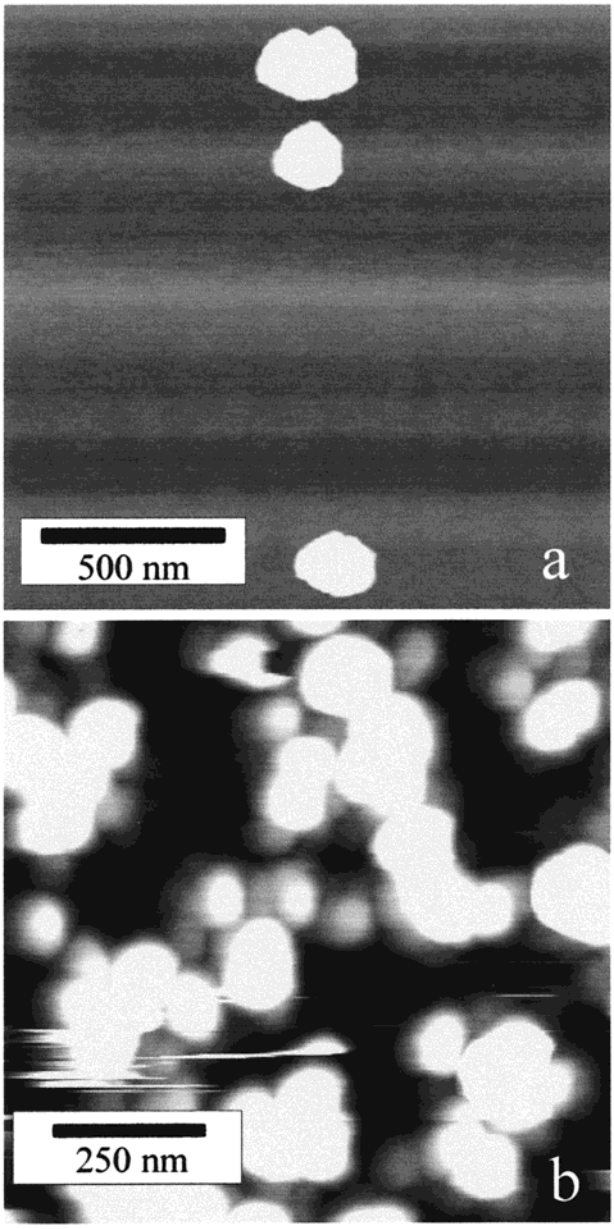


**Figure 10.** Height images of polystyrene latex spheres adsorbed to a mica surface from solutions of (a) 4.3 ppm and (b) 43 ppm.

The vertical heights of the adsorbed latex particles were measured from the height images of the particles. Given that the latex particles are nondeformable, the vertical height measured should be a true measure of particle diameter. The average vertical heights of the adsorbed latex particles measured by the AFM was 29 ± 5 nm, which is in good agreement with the manufacturer-quoted $R_H$ figure of 27 nm as measured by DLS. This result confirms the accuracy of the AFM height measurements of adsorbed particles, indicating that the measured vertical heights of the DMA−MMA structures should also be accurate.

**Effect of pH on the Adsorption of DMA−MMA Copolymer Solutions.** In Figure 11, images of the structures formed by the adsorbed DMA−MMA copolymer on mica as a function of pH and time are shown. When initially prepared, a solution of 500 ppm DMA−MMA has a natural pH of approximately 8.3. The other samples measured here were prepared by adding small amounts of acid to the sample to lower the pH. Considering the

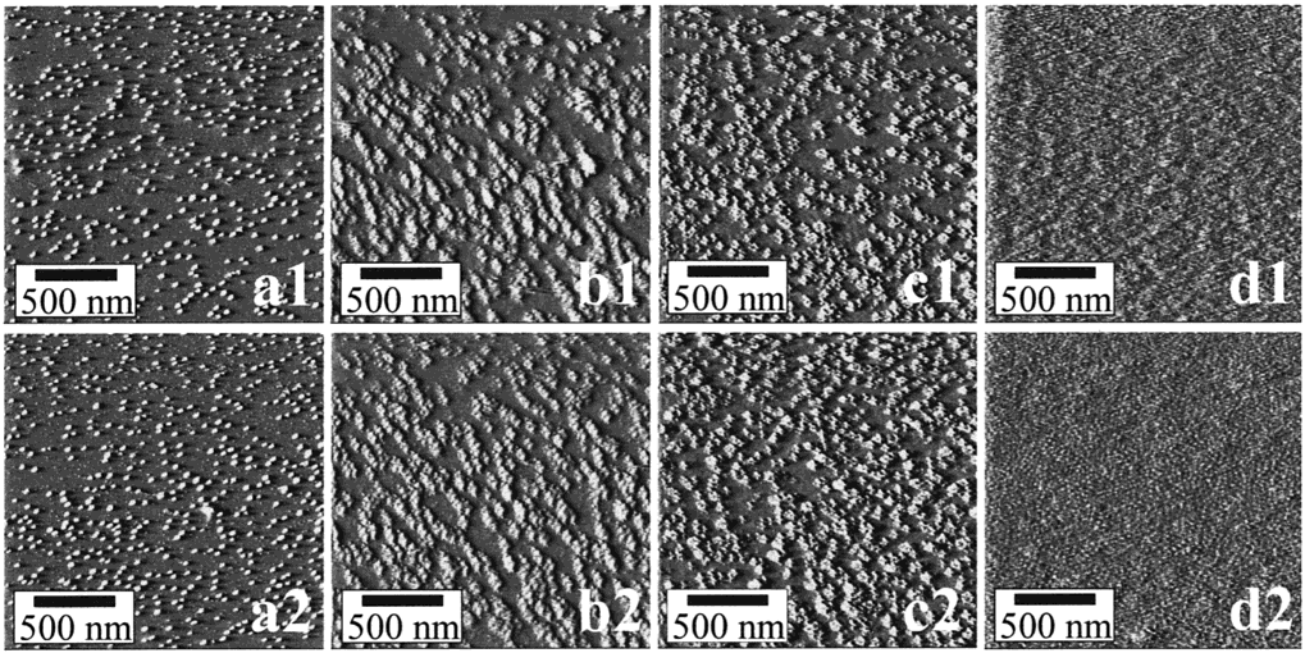


**Figure 11.** Images of the adsorbed layer of DMA−MMA copolymer adsorbed onto mica from 500 ppm copolymer solutions of various pH values. Images are from (a) pH 5, (b) pH 6, (c) pH 7, and (d) pH 8.3 (unadjusted pH) solutions. Images labeled a1−d1 were taken 1 h into the experiment, and images labeled a2−d2 were taken after 5 h.

**Table 1. Dimensions of the Aggregates in the Adsorbed Layer from, and in the Bulk Solution of, 500 ppm DMA−MMA Solutions at Various Values of pH, As Measured by AFM and DLS, Respectively**

| pH | method | vertical height (nm) | horizontal radius (nm) | hydrodynamic radius, $R_H$ (nm) | aggregate volume ($nm^3$) |
|---|---|---|---|---|---|
| 4 | AFM | 5.2 ± 1.3 | 36.3 ± 14.8 | | $1.09 \times 10^4$ |
| | DLS | | | 30.46 ± 0.86 | $1.18 \times 10^5$ |
| 5 | AFM | 5.0 ± 2.3 | 37.6 ± 10.0 | | $1.12 \times 10^4$ |
| | DLS | | | 25.96 ± 0.22 | $7.33 \times 10^4$ |
| 6 | AFM | 3.0 ± 0.26 | 78.1 ± 25.4 | | $2.87 \times 10^4$ |
| | DLS | - | - | 26.77 ± 0.55 | $8.04 \times 10^4$ |
| 7 | AFM | 4.1 ± 1.1 | 89.4 ± 46.3 | | $5.17 \times 10^4$ |
| | DLS | | | 24.52 ± 0.66 | $6.17 \times 10^4$ |
| 8.3 (unadjusted) | AFM | *a* | *a* | | |
| | DLS | | | 16.10 ± 0.32 | $1.75 \times 10^4$ |

[a] The dimensions of aggregates adsorbed from a solution at natural pH conditions could not be measured using the AFM since the aggregates do not adsorb as discrete units.

images collected at the four pH values below the natural conditions, Figure 5 and Figure 11a−c, it is apparent that all samples show a random pattern of adsorbed structures. These structures in the adsorbed layer below the natural pH are believed to be domes of the MMA cores protruding from the surrounding DMA layer. The apparent morphologies of the domes change with the pH of the copolymer solution. The domes appear to become broader and less uniform in size as the pH is increased. There is no accompanying significant change in the apparent dome height. The dimensions of the MMA domes imaged in the adsorbed layers from solutions of various pH values are given in Table 1. The dimensions of the MMA domes in the adsorbed layers must be treated with caution. At pH 6 and 7, the MMA domes appear less monodisperse in size and less regular in morphology when compared to the MMA domes imaged in the pH 4 and 5 solutions. Also of note is that the surface coverage of the MMA domes at any given time increases significantly as the pH is increased. At pH 7 the surface density at low time scales (Figure 11, c1) is higher than the pH 4 solution at 22 h.

Images of the adsorbed layer of DMA−MMA from a solution where the pH was not adjusted, Figure 11d, are quite different from those where the pH was adjusted. When the pH was not adjusted, the adsorbed layer shows little or no surface morphology at short time periods (Figure 11, d1); however, as the experiment continues, the surface begins to exhibit zones of an ordered close-packed sphere morphology (Figure 11, d2). The differences in the adsorbed layer as the pH of the solutions changes can be due to either changes in the solution morphology of the DMA−MMA micelles or changes associated with copolymer adsorbed to the mica surface.

To investigate which of the two above possibilities is responsible for the observed change in the adsorbed copolymer layer, the hydrodynamic radii of the DMA−MMA copolymer micelles in the bulk 500 ppm solutions of various pH values were measured using DLS, as shown in Table 1. The hydrodynamic radius of the micelles does indeed change as a function of the pH of the solution; however, the change is opposite to the observed trend in the dimensions of the structures in the adsorbed layer. The hydrodynamic radius of DMA−MMA micelles decreases as the pH increases from 4 to 5 and then changes little as pH increases from 5 to 7. A further decrease in the hydrodynamic radius is observed when the DMA−MMA solution is left at its natural pH. The change in $R_H$ as a function of pH is easily explained when one considers the DMA block of the copolymer. At pH 4, the DMA is highly charged due to the tertiary amine groups associat-

ing a proton, causing micellization as described earlier. The high charge on the DMA blocks leads to the corona of the micelle being extended, since there is a large electrostatic repulsion between the DMA blocks in the corona. As the pH is increased, the charge on the DMA blocks is decreased, and so the electrostatic repulsion between the blocks is similarly decreased, allowing the micelle corona to collapse. In a solution where the pH is unadjusted, the DMA blocks still carry enough residual charge to allow micellization of the DMA−MMA copolymer, although the low charge means the corona of the micelle is in a highly collapsed state.

The proposed model of copolymer micelle adsorption can be used to understand the changes in the morphology of the adsorbed DMA−MMA layer observed as the pH of the bulk solution changes. Hartley et al.[55] have measured the zeta-potential of a mica surface using a streaming potential apparatus in an aqueous solution of $10^{-4}$ M $NaNO_3$. They found the zeta-potential of mica to be approximately −30 mV at pH 4, increasing to approximately −75 mV as the pH was increased to 7, and then remaining essentially constant as the pH rose further. It should be noted here that at the start of each experiment water adjusted to the pH of the copolymer solution to be studied was injected into the fluid cell to record force−distance data and an image of the bare mica surface. The water was then left for 20−30 min to allow the mica surface to equilibrate to the pH of the copolymer solution. Thus, as the pH of the copolymer solution increased from 4 to 7, the negative charge of the mica surface to which the DMA−MMA was adsorbing also increased. An immediate effect of this is that as the pH of the bulk copolymer solution is increased the micelles may be expected to adsorb more rapidly in the initial stages. Evidence of this can be seen clearly from the images in Figures 5 and 11, with more MMA domes apparent in images taken at both 1 and 5 h as the pH of the adsorbing solution is increased. This in turn leads to greater steric crowding at the surface and a hindered relaxation mechanism for the coronal DMA chains, allowing the copolymer micelles to adsorb in closer proximity to each other.

The apparent changes in the morphology of the MMA domes protruding from the adsorbed DMA layer can also be explained by the proposed model of adsorption. When a polyelectrolyte adsorbs to a surface of opposite charge, it does so with a loop and train conformation, in which trains of the polyelectrolyte are adsorbed to the surface and loops of unadsorbed polyelectrolyte extend into solution.[1] A polyelectrolyte of low charge density adsorbs to a charged surface with longer loops and shorter trains relative to a polyelectrolyte of higher charged density. This difference in these two conditions is shown schematically in Figure 12. As a result of the difference in conformation, the loops of the adsorbed brush layer for a low charge density polyelectrolyte adsorbed at a surface are more flexible than the brush layer of a polyelectrolyte of higher charge density. This is due to the decreased electrostatic repulsion between the loops as a consequence of the lower charge density. In this way the loops of a low charge density polyelectrolyte are "softer" in an imaging sense, with polymer chains able to move and compress as the AFM tip passes over them.

As the pH of the bulk solution is increased, the charge density on the DMA chains is reduced, since fewer of the tertiary amines are protonated, as evidenced by the reduction in the DMA−MMA micelle size in solution.

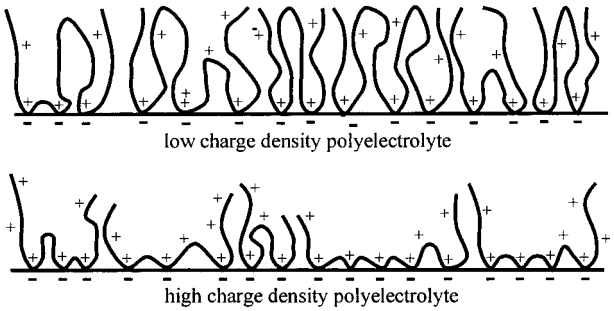


**Figure 12.** Schematic representation of the different conformations of polyelectrolytes of different charge densities adsorbed to a charged surface.

Consequently, the layer of DMA coronal chains adsorbed to the surface adopts a more extended loop conformation as the pH of the bulk solution is increased, and the brush layer becomes "softer" in an imaging sense. As the layer of DMA becomes "softer", the contrast between this layer and the MMA domes protruding from the layer decreases, resulting in a decrease in the definition image of the adsorbed layer. Another complicating factor is the increased possibility of the DMA−MMA copolymer adsorbing to the cantilever tip as the charge on the copolymer is decreased. Any adsorption to the tip will also decrease the definition in the AFM image.

The above arguments explain the differences in the adsorbed layer morphology when the DMA−MMA is adsorbed from solutions at pH values lower than the natural conditions. In the case of the copolymer adsorbed from a solution where the pH has not been adjusted (pH ∼8.3), the surface is highly negatively charged, whereas the positive DMA blocks on the copolymer are only weakly charged. However, enough charge exists to allow the formation of micelles and prevent precipitation of the copolymer chains. When the copolymer solution is injected into the fluid cell of the AFM, the DMA−MMA micelles form an adsorbed layer that is quite unlike those seen for the lower pH solutions. Images of the adsorbed layer taken soon after the injection of the solution do not reveal any features due to the inability to maintain a stable interaction between the tip and the surface. As the imaging force stabilizes, the morphology of the adsorbed layer begins to become apparent. The images reveal a random distribution of circular structures over the entire surface, and while the layer does not exhibit a true close-packed distribution, the structures are more densely packed than in the lower pH cases. Two-dimensional fast Fourier transforms were performed on images of the adsorbed layer, though analysis was hampered by the low order of the adsorbed structures, providing a peak-to-peak distance of between 30 and 70 nm. This equates to an effective "footprint" radius for each adsorbed aggregate of between 15 and 35 nm, which is approximately half that calculated for the DMA−MMA micelles adsorbed from a pH 4 solution. More importantly, this calculated surface "footprint" is in the range of the measured hydrodynamic radius for DMA−MMA in a solution at natural conditions. The close packing of the DMA−MMA micelles at natural pH conditions is due to the hindered relaxation of the DMA chains after micellar adsorption has occurred. The relaxation of the coronal DMA chains is retarded in two ways. First, the high surface charge results in rapid electrostatic adsorption of the DMA−MMA micelles from solution, which decreases the time in which the coronal chains can relax before the adsorption of other micelles from solution. Compounded with this is the fact that the low charge density of the DMA results in the chains experiencing

(55) Hartley, P. G.; Larson, I.; Scales, P. J. *Langmuir* **1997**, *13*, 2207−2214.

poor solvation conditions, and thus coronal expansion is slowed, resulting in less relaxation before the adsorption of further micelles from solution.

## Conclusions

The adsorption of the homopolymer poly(2-(dimethylamino)ethyl methacrylate) (DMA) at the solution/mica interface was studied using in situ atomic force microscopy. Images of the adsorbed DMA layer taken under a range of concentrations revealed a featureless layer, with no evidence of adsorbed structures. Force−distance data revealed that charge neutralization of the negatively charged mica surface occurred when the DMA was adsorbed from a solution at 10 ppm concentration. However, when the DMA was adsorbed from a solution at 250 ppm concentration force−distance data indicated that charge reversal had occurred, resulting in a positively charged adsorbed layer.

The adsorption of the amphiphilic diblock copolymer poly(2-(dimethylamino)ethyl methacrylate-*block*-methyl methacrylate) (DMA−MMA) at the solution/mica interface was also investigated using in situ atomic force microscopy. Images taken when the copolymer is adsorbed from a 500 ppm solution at pH 4 reveal adsorbed layers with discrete, monodisperse structures. These surface structures have a much lower volume than the copolymer micelles have in solution. Force−distance data measured normal to the surface in the regions between these structures indicate that adsorption of positively charged material has also occurred in these areas. It is proposed that the DMA−MMA copolymer adsorbs to the mica surface as individual micelles. Once the micelle has adsorbed to the surface, the charged DMA coronal chains of the micelle relax and adsorb to the surface via electrostatic attractions. In this way, the adsorbed layer of the copolymer can be thought of as a layer of DMA chains, with the observed surface structures being the glassy MMA cores protruding through the layer. These protruding MMA cores are then revealed as domes on an otherwise featureless adsorbed layer.

Images of the adsorbed layer over a 22 h period reveal an increase in the number of MMA domes as the experiment progresses; however, a simple counting method reveals that the rate of increase in the number of MMA domes decreases over time. These data support the proposed mechanism of copolymer adsorption, in which the diblock copolymer micelles are directly adsorbed onto the mica surface. The relaxation of the coronal chains decreases the number of free charged sites on the mica, thereby decreasing the available sites for adsorption of further DMA−MMA micelles from solution. In this way the rate of adsorption for the DMA−MMA micelles decreases as the experiment continues.

As the pH of the copolymer solution is increased, the charge density on the mica surface increases. This allows more rapid adsorption of micelles, which in turn decreases the time for the coronal chains to relax onto the surface, resulting in the copolymer micelles adsorbing closer together. Also, as the pH of the solution is increased, the charge density on the DMA chains is decreased. As a consequence, the DMA layer becomes "softer" in an imaging sense, and the contrast between the DMA layer and the MMA domes decreases. This results in lower definition between the DMA layer and the MMA cores in the AFM images taken of the adsorbed layer as the pH of the bulk solution is increased from 4 to 7.

When the copolymer micelles are adsorbed from a solution at natural pH, initial images reveal a featureless layer. However, once the imaging force has stabilized, images reveal that micelles have adsorbed randomly over the entire surface. The average peak-to-peak distance of the adsorbed micelles in this case is in the range of the micelle hydrodynamic radius in a solution at natural pH, indicating that the micelles have adsorbed in a manner near to a close-packed sphere morphology. The higher surface density of adsorbed micelles under these conditions is due to the hindered relaxation of the DMA coronal chains to the mica surface. This retardation of the relaxation mechanism is due in part to the lower charge density of the DMA chains, which creates poor solvation conditions and thus impedes coronal expansion, and also to the higher rate of micellar adsorption which decreases the time allowed for the coronal chains to relax.

In contrast to the adsorption of the DMA−MMA micelles, in which the molecular freedom of the coronal chains hinders adsorption of the micelles in close proximity, is the adsorption of latex particles. Nondeformable, positively charged latex spheres were used to investigate the role of molecular freedom in adsorption. It was found that the latex particles achieved entire surface coverage, in a random close-packed adsorbed layer, at concentrations much lower than those used in the copolymer micelle experiments. This is logical, since the latex particles cannot undergo any form of relaxation and thus do not use any charged sites on the surface other than those used in the initial adsorption. Images of the adsorbed latex spheres most closely resemble the DMA−MMA copolymer adsorbed layer when the copolymer is adsorbed under natural pH conditions. In these conditions the relaxation of the DMA coronal chains is hindered by the high charge density of the mica surface and the low charge density of the DMA coronal chains. This result supports the proposed hypothesis that the relaxation of the DMA coronal chains, once the DMA−MMA micelle has adsorbed to the mica surface, plays a significant role in determining the adsorbed layer morphology for the adsorption of DMA−MMA copolymer to a mica surface.

LA010335+